ISBN: 978-3-95450-250-9 ISSN: 2673-5520 doi:10.18429/JACoW-MEDSI2023-TUPYP048

A HIGH REPETITION RATE FREE-ELECTRON LASER SHUTTER SYSTEM

Jiacheng Gu, Yajun Tong†, Zhen Wang, Huaidong Jiang
School of Physical Science and Technology, ShanghaiTech University, Shanghai, China

Abstract

The Shanghai High repetition rate XFEL and Extreme light facility (SHINE) is the first high repetition rate XFEL in China. It is a powerful tool for scientific research. The high repetition rate XFEL has not only high peak power but also high average power. The high average power will cause the distortion of optics and make the diagnostics failure. To measure the distortion of optics, the diagnostics, such as wavefront sensor, imager, should be working properly. A fast shutter system is designed to protect the diagnostics and to make the diagnostics working properly. It can control the number of pulses and average power on the diagnostics. The time window of shutter can be as small as 10 milliseconds. It can absorb most of FEL power.

INTRODUCTION

X-ray free electron laser (XFEL) is a new generation of advanced light source based on particle accelerators, with excellent characteristics such as ultra-short pulses, ultra-high brightness, high coherence, and continuously adjustable output wavelength. It has made significant progress in the past decade [1], and the XFEL facility has also become a powerful tool for cutting-edge research in life sciences, materials science, physics, and other fields [2]. The Shanghai High repetition rate XFEL and Extreme light facility (SHINE) is the first hard X-ray free electron laser facility in China, with a maximum electron energy of 8 GeV and a maximum repetition rate of 1 MHz. In the phase-I, it offers a photon energy range of 0.4-25 keV. SHINE's accelerator parameters are listed in Table 1 [3].

However, high repetition rate XFEL has both peak power and average power, and its high peak power can cause damage to the devices in the optical path. High average power can bring thermal load on the devices and cause thermal distortion to the optics, affect the beam transportation and focusing, and cause diagnostics failure. Therefore, how to diagnostics the distorting beam under high repetition rate is particularly important.

M. Renier and colleagues previously designed an X-ray shutter for the European Synchrotron Radiation Facility (ESRF) [4]. It can control the shortest exposure time achieved 3 milliseconds. However, it was not suitable for operation under high vacuum conditions. In a different endeavour, Chang Yong Park and collaborators designed a shutter tailored for high vacuum environments [5]. Their shutter realized the use of vacuum environment but their stopper cannot withstand 100W laser's heat load for a long time. To address this critical need, we have designed a shutter system based on M. Renier's design, but it can work in vacuum. The shutter's aperture is 4mm which is suitable for the small beam size of hard X-ray beamline, with a minimum time window of 10 milliseconds. To ensure efficient heat conduction within the stoppers and free falling, liquid metal is employed for cooling purposes.

Table 1: The Main Parameters of SHINE

Parameters	Nominal	Objective
Beam energy [GeV]	8	4~8.5
Bunch charge [pC]	100	10~300
Peak current [kA]	1.5	0.5~3
Slice emittance [μm·rad]	0.4	0.2~0.7
Max repetition rate [MHz]	1	1
Beam power [MW]	0.8	0~2.4
Photon energy [keV]	0.4~25	0.2~25
Pulse length [fs]	66	3~600

SHUTTER DESIGN

Basic Principle of the Device

The shutter consists of two sandwiched stoppers, as illustrated in Fig. 1. Each stopper is guided to move linearly along a track and is driven by a combination of an electromagnet and its own gravity. The system operates in the following states:

(a) State 1: In this configuration, both stoppers are positioned at their lowest point, and they are actively cooled. Notably, stopper 1 is responsible for absorbing the thermal load.

(b) State 2: When the need arises to create an time window, both stoppers are raised to their highest position, and at this point, neither receives cooling. This state typically lasts for less than 1 second.

(c) State 3: The electromagnets of the two stoppers begin to fall at different time, forming a defined time window. Eventually, both stoppers return to their lowest position, effectively reverting to the configuration of State 1.

The stopper is designed as a sandwich structure, comprised of three key components: a radiation damage resistant block (diamond), a burn-through detector, and a tungsten block, as depicted in Fig. 2. The burn-through detector serves the purpose of identifying whether the radiation damage resistant block has experienced burn-through. Its fundamental operational principle relies on the interaction of incident light with a YAG crystal, resulting in the generation of visible fluorescence. A photodiode is employed to detect this optical signal, which is subsequently transmitted as an interlocking signal through the connecting lead wire. Meanwhile, the tungsten block is deployed

† tongyj@shanghaitech.eud.cn

ISBN: 978-3-95450-250-9 ISSN: 2673-5520 doi:10.18429/JACoW-MEDSI2023-TUPYP048

to ensure that no photons can pass through the shutter, thus reinforcing its protective function. radiation damage resistant block should be designed to be removable, allowing for replacement once it has been burned through.

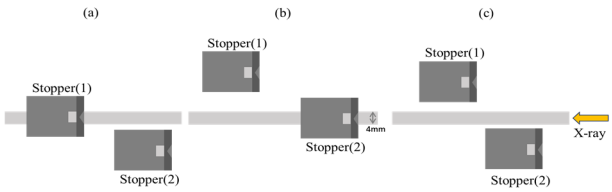

Figure 1: Principle of operation.

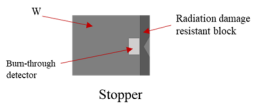

Figure 2: The composition and structure of the stopper

As illustrated in Figs. 3(a) and 3(b), the actuation of the stopper is achieved through a combination of a solenoid-type electromagnet, and gravity. Stoppers rise by electromagnetic force and fall by gravity. A guide rail ensures the linear motion of the device, while the spring serves to impact forces at the end of the stopper's stroke. As the stopper enters the water-cooled tank, its lower surface makes initial contact with a reservoir of liquid In-Ga. A section of the stopper is submerged in this liquid, thereby enhancing the heat exchange efficiency between the stopper and the water-cooled tank. Ultimately, heat is conducted out of the vacuum environment through the cooling water within the vacuum water pipe. The welding flange of each individual stop device is connected to the chamber flange. A heat sink is deployed to enhance the heat dissipation efficiency of the outer solenoid coil. The upper edge of the heat sink is welded to the stationary iron core, while the lower edge is welded to the welding flange, preserving the vacuum integrity of the chamber environment.

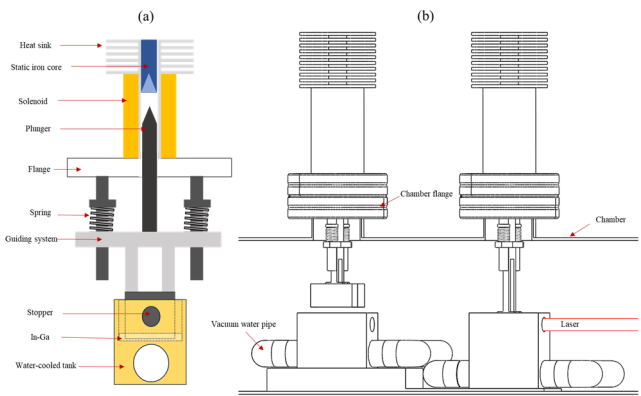

Figure 3: Shutter structure. (a) schematic diagram of key driving principles (b) actual drive plan structure assembly drawing.

SHUTTER SIMULATION

Finite Element Analysis of Thermal Load

Given the substantial thermal load absorbed by the stopper, a crucial element in its reliable operation is the use of high thermal conductivity liquid indium gallium for effective heat dissipation. In this system, heat is efficiently transferred from the stopper to a copper tank by means of the liquid In-Ga. Subsequently, the heat is exchanged with the copper tank through a water-cooled tube, facilitating the transfer of heat to the exterior of the chamber. This designed process enables vacuum cooling, ensuring the maintenance of ideal operating conditions.

Theory And Model

In our analysis of the key component, the stopper, we employed simulation software. Initially, we chose diamond as the damage-resistant block and B_4C was used as a comparison. As depicted in Fig. 4b, the fundamental model structure involved a laser beam with a total power of 100 W and a half-height width of 1.41 mm, adhering to a standard Gaussian distribution. The heat generated was deposited on the surface of the diamond and subsequently diffused into the heavy metal tungsten block. Concurrently, heat was transferred into the copper water-cooled channel, which exhibits high thermal conductivity, through the liquid In-Ga. Ultimately, the heat within the copper was conveyed out of the vacuum environment through water flow, enabling efficient heat dissipation. The final mesh division results are showcased in Figs. 4(c) and 4(d).

In this model, we set the centre of the beam at the surface as the beam origin O(0,0,0), the beam direction e(0,0,-1), and refer to Fig. 4c for the coordinate system. The light source follows a Gaussian distribution:

$$f(O,e) = \frac{1}{2\pi\sigma^2}\exp\left(-\frac{d^2}{2\sigma^2}\right), d = \frac{\|e \times (x-O)\|}{\|e\|} \quad ,$$

where, $\sigma = 0.6$ mm.

When a high repetition frequency free electron laser irradiates a material, the energy absorbed by the material is deposited inside the material, and the final energy diffuses in the form of thermal energy inside the material, following the thermal conduction law. In the three-dimensional coordinate system of the HT module, the classical Fourier heat transfer equation expression is:

$$\begin{aligned}\rho(T)C_P(T)\cdot\partial T(x,y,z,t)/\partial t &= \partial/\partial x\,(k(T)\cdot\partial T(x,y,z,t)/\partial x)\\ &+ \partial/\partial y\,(k(T)\cdot\partial T(x,y,z,t)/\partial y)\\ &+ \partial/\partial z\,(k(T)\cdot\partial T(x,y,z,t)/\partial z)\\ &+ Q(x,y,z,t),\end{aligned}$$

where $T(x,y,z,t)$ is the variation of temperature over time and space, $\rho(T), C_P(T), k(T)$ are functions of material density, constant pressure heat capacity, and thermal conductivity. $Q(x,y,z,t)$ is the heat source converted from laser to the material. The detailed parameters are shown in Table 2.

ISBN: 978-3-95450-250-9 ISSN: 2673-5520 doi:10.18429/JACoW-MEDSI2023-TUPYP048

Table 2: The Main Parameters of Material

Material	ρ (kg/m^3)	C_P $(J/kg \cdot K)$	k $(W/m \cdot K)$
Diamond	3515	516	2500
Copper	8960	385	400
In-Ga	6440	420	28
B_4C	2520	20-2000	14-32

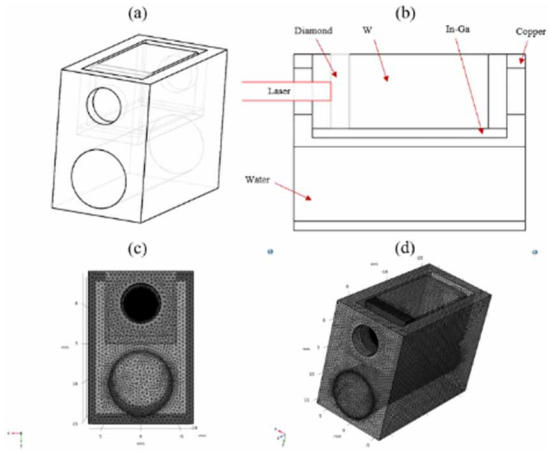

Figure 4: Block structure. (a) structure diagram, (b) half sectional detailed structure, (c) front view, (d) side view.

Result

Under steady-state conditions with a water flow rate of 0.33 litters per minute, the highest temperature observed on the diamond surface is 114 °C, the highest temperature on the tungsten surface is 97 °C, and the highest temperature on the liquid In-Ga surface is 91 °C (Fig. 5). These temperatures fall within the reasonable range for these materials. Taking into account cost considerations, a comparative analysis was conducted to assess the impact of different radiation damage resistant materials on the overall equipment performance. Specifically, 2 mm thick B_4C and 2 mm thick diamond were compared. Notably, B_4C exhibits significantly lower thermal conductivity than diamond. Under steady-state conditions with a water flow rate of 0.33 litters per minute, the highest surface temperature reached 1800 °C when B_4C was use (Fig. 6). This result indicates that B_4C's heat dissipation performance is less effective than that achieved with diamond.

CONCLUSION

To ensure the proper operation of diagnostic equipment for the high repetition rate FEL, we have designed a spiral tube-driven shutter. All materials used in the shutter are compatible with high vacuum conditions. Through careful design of the stopper, the heat dissipation system, and the driving mechanism, it is expected to meet the requirements for long-term usage and with a minimum 10-millisecond window.

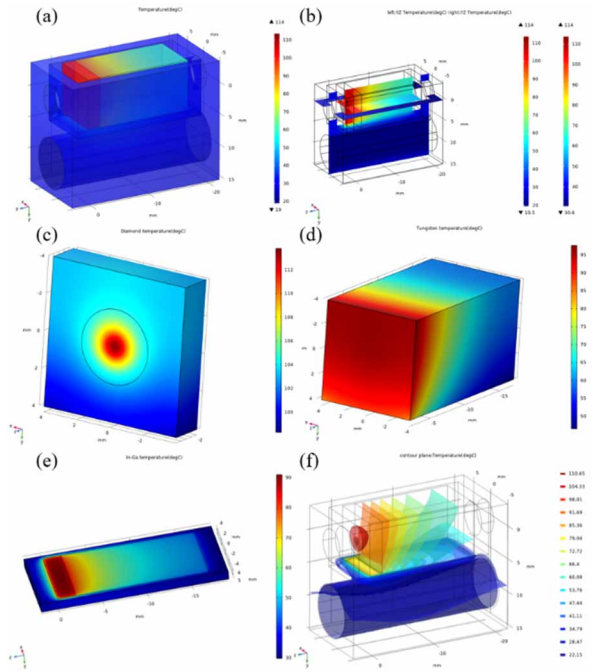

Figure 5: 2 mm thick Diamond with steady state temperature at a water flow rate of 0.33 L/min. (a) surface temperature distribution, (b) profile temperature distribution map, (c) diamond temperature distribution, (d) tungsten temperature distribution, (e) liquid indium gallium temperature distribution, (f) temperature contour map.

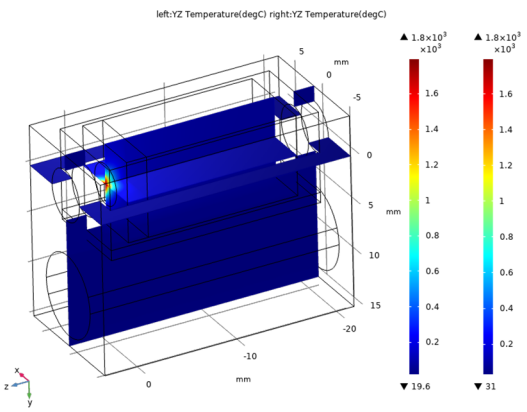

Figure 6: 2 mm thick B_4C with steady-state temperature at a water flow rate of 0.33 L/min.

REFERENCES

[1] P. Emma *et al.*, "First lasing and operation of an angstrom-wavelength free-electron laser", *Nat. Photonics*, vol. 4, p. 641-647, 2010. doi:10.1038/Nphoton.2010.176

[2] H. N. Chapman, "X-Ray Free-Electron Lasers for the Structure and Dynamics of Macromolecules", *Annu. Rev. Biochem.*, vol. 88, p. 35-58, 2019. doi:10.1146/annurev-biochem-013118-110744

[3] Z. Zhu, Z. T. Zhao, D. Wang, Z. H. Yang, and L. Yin, "SCLF: An 8-GeV CW SCRF Linac-Based X-Ray FEL Facility in Shanghai", in *Proc. FEL'17*, Santa Fe, NM, USA, Aug. 2017, pp. 182-184. doi:10.18429/JACoW-FEL2017-MOP055

ISBN: 978-3-95450-250-9 ISSN: 2673-5520 doi:10.18429/JACoW-MEDSI2023-TUPYP048

[4] M. Renier *et al*., "A white-beam fast-shutter for microbeam radiation therapy at the ESRF", *Nucl. Instrum. Methods Phys. Res., Sect. A,* vol. 479, no. 2-3, pp. 656-660, 2002. doi:10.1016/S0168-9002(01)00905-6

[5] C. Y. Park *et al*., "Ultra-high vacuum compatible full metal atom beam shutter for optical lattice clocks", *Rev. Sci. Instrum.,* vol. 94, p. 013201, 2023. doi:10.1063/5.0123971